

Competing d_{xy} and s_{\pm} Pairing Symmetries in Superconducting $\text{La}_3\text{Ni}_2\text{O}_7$ emerge from LDA+FLEX Calculations

Griffin Heier¹, Kyungwha Park², Sergey Y. Savrasov¹

¹*Department of Physics, University of California, Davis, CA 95616, USA and*

²*Department of Physics, Virginia Tech, Blacksburg, Virginia 24061, USA*

(Dated: December 8, 2023)

With recent discoveries of superconductivity in infinite-layer nickelates, and in $\text{La}_3\text{Ni}_2\text{O}_7$ under high pressure, new opportunities appeared that yet another family of high-temperature superconductors based on Ni element may exist in Nature as was previously the case of cuprates and iron based materials. With their famous strong Coulomb correlations among 3d electrons and the proximity to antiferromagnetic instability these systems represent a challenge for their theoretical description, and most previous studies of superconductivity relied on the solutions of simplified few-orbital model Hamiltonians. Here, on the other hand, we use a recently developed combination of density functional theory with momentum and frequency resolved self-energies deduced from the so-called Fluctuational-Exchange (FLEX)-type Random Phase Approximation (RPA) to study spin fluctuation mediated pairing tendencies in $\text{La}_3\text{Ni}_2\text{O}_7$ under pressure. This methodology uses first-principle electronic structures of an actual material and is free of tight-binding parametrizations employed in model Hamiltonian approach. Based on our numerical diagonalization of the BCS Gap equation we show that competing d_{xy} and s_{\pm} pairing symmetries emerge in superconducting $\text{La}_3\text{Ni}_2\text{O}_7$ with the corresponding coupling constants becoming very large in the proximity of spin density wave instability. The results presented here are discussed in light of numerous other calculations and provide on-going experimental efforts with predictions that will allow further tests of our understanding of unconventional superconductors.

PACS numbers:

Opportunities to realize high-temperature superconductivity have always been a subject of enormous research interest, and recent discoveries of superconducting nickelates[1, 2] is not an exception. Despite numerous theoretical and experimental efforts in the past [3–8], infinite-layer Nd_2NiO_2 were shown to exhibit superconductivity at 8K only a few years ago [1, 9, 10] but just discovered 80K superconductivity in bulk $\text{La}_3\text{Ni}_2\text{O}_7$ under applied pressures over 14GPa[2] has brought nickelates into focus of becoming a new addition to the famous family of high-temperature superconducting cuprates and ironates[12–14].

This breakthrough has inspired a large-scale theoretical effort to understand the nature of superconductivity in $\text{La}_3\text{Ni}_2\text{O}_7$. First principles electronic structure calculations based on Density Functional Theory (DFT) and Local Density Approximation (LDA)[18] reveal the dominant role of Ni $3d_{x^2-y^2}$ orbitals and, in addition, of Ni $3d_{3z^2-r^2}$ orbitals [2, 16, 17]. Correlation effects beyond DFT have been studied [19–21] using combinations of LDA and GW methods with dynamical mean field theory (LDA+DMFT and GW+DMFT)[15]. Two-orbital bilayer models for the bands near the Fermi level have been proposed to describe the low energy physics of this material [22, 23]. Many-body simulations of model Hamiltonians with Quantum Monte Carlo[24] and density matrix renormalization group[25] techniques have also recently appeared.

Focusing on the superconducting state, the s_{\pm} pairing symmetry with sign changing order parameter on

different sheets of the Fermi surface has been put forward in a series of recent works[19, 20, 22, 26–31]. Such calculations frequently rely on the so-called spin fluctuational mechanism of superconductivity that has been proposed to understand properties of heavy fermion systems many years ago [32, 33]. Diagrammatically, this includes particle-hole ladder and bubble diagrams and is known as Random Phase Approximation (RPA) [34, 35]. The inclusion to these series of particle-particle ladder diagrams has also been proposed in the past, which was entitled as the Fluctuational Exchange Approximation (FLEX) [36]. This contribution was however found to be not essential in the proximity to magnetic instability where the most divergent terms are described by the particle-hole ladders[37].

We have recently implemented a combination of density functional electronic structure theory with momentum- and energy-dependent self-energy deduced from the above mentioned FLEX-RPA method[38]. This LDA+FLEX(RPA) approach evaluates dynamical charge and spin susceptibilities of the electrons in a Hilbert space restricted by correlated orbitals only, similar to popular LDA+U[40] and LDA+DMFT approaches[15]. Evaluations of superconducting pairing interactions describing scattering of the Cooper pairs at the Fermi surface in a realistic material framework became possible using this method. Our most recent calculations of $\text{HgBa}_2\text{CuO}_4$ [39], a prototype single-layer cuprate superconductor, where a much celebrated $d_{x^2-y^2}$ symmetry of the order parameter was easily recovered with

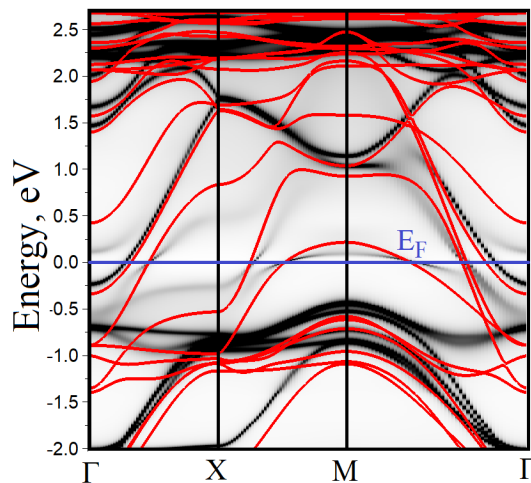


FIG. 1: Electronic structure of $\text{La}_3\text{Ni}_2\text{O}_7$ with lattice parameters corresponding to pressure 30 GPa calculated using DFT+FLEX method (black) with $U=3$ eV and $J=0.5$ eV, as well as the result of density functional calculation (red).

LDA+FLEX, has demonstrated applicability of this method to study spin-fluctuation mediated superconductivity without reliance on tight-binding approximations of their electronic structures.

Here we apply the LDA+FLEX method to study superconductivity in bulk $\text{La}_3\text{Ni}_2\text{O}_7$ under pressure. Our calculated normal-state self-energies for Ni 3d-electrons show a very strong frequency dependence and at the same time rather weak momentum dependence with the electronic mass enhancement m/m_{LDA} of the order of 4 in close proximity to the spin density wave instability. Our numerically evaluated superconducting pairing interaction describing scattering of the Cooper pairs at the Fermi surface is used to exactly diagonalize the linearized Bardeen-Cooper-Schrieffer (BCS) gap equation on a three dimensional \mathbf{k} -grid of points in the Brillouin Zone. The highest eigenstate deduced from this procedure represents a spin fluctuational coupling constant λ similar to electron-phonon λ in conventional theory of superconductivity. The spin fluctuational λ was found to be very sensitive to the actual values of the Hubbard interaction U among Ni 3d electrons serving as input to this calculation but reaches rather large values in close proximity to spin density wave instability. The most interesting result is that the superconducting order parameter is predicted to be of d_{xy} symmetry for the most relevant range of values of U while the recently proposed s_{\pm} symmetry emerges as the second closest eigenstate. This is quite unusual in light of $d_{x^2-y^2}$ pairing state being found in cuprates[41] and of s_{\pm} pairing in ironates. Due to the appearance of nodes in d_{xy} and its absence in s_{\pm} symmetry the on-going experimental efforts should easily elucidate which pairing symmetry is realized here.

A unit cell of bulk $\text{La}_3\text{Ni}_2\text{O}_7$ contains two Ni-O planes

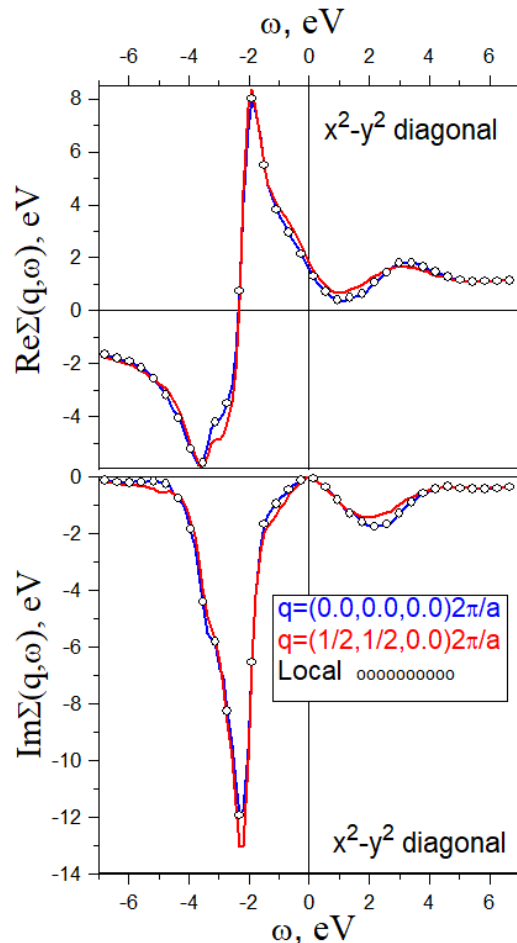


FIG. 2: Calculated self-energy $\Sigma(\mathbf{k}, \omega)$ (top is the real part, and bottom is imaginary part) using FLEX-RPA approximation for $d_{x^2-y^2}$ electrons of Ni in $\text{La}_3\text{Ni}_2\text{O}_7$. The wavevectors \mathbf{k} correspond to (000) and $(\frac{1}{2}, \frac{1}{2}, 0)$ of the Brillouin Zone. The circles show the result of the local self-energy approximation taken as the average over all \mathbf{k} -points. A representative value of Hubbard $U=3$ eV and $J=0.5$ eV is used.

and is expected to have its orthorhombic structure with space group $Fmmm$ [42]. This is also true under applied pressure[2]. At 30 GPa, the theoretically deduced lattice parameters are given by: $a = 5.29\text{\AA}$, $b = 5.21\text{\AA}$, $c = 19.73\text{\AA}$. We perform our density functional electronic structure calculations [18] using the full potential linear muffin-tin orbital method [43]. The self-energies for Ni 3d electrons, $\Sigma(\mathbf{k}, \omega)$, are evaluated on the $12 \times 12 \times 12$ grid of \mathbf{k} -points and at the frequency range between -13.6 eV and $+13.6$ eV from the Fermi energy based on RPA-FLEX procedure described previously[38, 39]. We use the values of an on-site Hubbard interaction $U = 3$ eV and $J = 0.5$ eV as an input to the simulation similarly to Ref. [22].

Since the self-energy has both real and imaginary parts, the electronic states do no longer have infinite life

times. We evaluate the poles of the single particle Green function, and the obtained $\text{Im}G(\mathbf{k}, \omega)$ for $\text{La}_3\text{Ni}_2\text{O}_7$ is shown in Fig. 1. The Fermi surface states mainly consist of Ni $3d_{x^2-y^2}$ and Ni- $3d_{3z^2-r^2}$ orbital character. There is a small La based pocket seen around the Γ point but it should be irrelevant for the superconducting behavior of $\text{La}_3\text{Ni}_2\text{O}_7$. Most of the poles are seen as sharp resonances (plotted in black) in the function $\text{Im}G(\mathbf{k}, \omega)$ that closely follows the LDA energy dispersions (plotted in red). However, the difference is seen in the behavior of the Ni $3d_{x^2-y^2}$ and Ni- $3d_{3z^2-r^2}$ states in the vicinity of the Fermi surface that acquire a strong damping at energies away from the Fermi level. As the primary effect of the self-energy is the renormalization of the electronic bandwidth, we found the electronic mass enhancement to be around 3.4 for Ni $3d_{x^2-y^2}$ and 4.7 for Ni $3d_{3z^2-r^2}$ orbitals.

We further plot the diagonal elements of the real and imaginary parts of the self-energy for Ni $3d_{x^2-y^2}$ orbital in Fig.2. To illustrate the \mathbf{k} -dependence we show the result for the two points of the Brillouin Zone (BZ): $\Gamma = (0, 0, 0)$ (blue) and $M = (1/2, 1/2, 0)$ (red). We generally find the \mathbf{k} -dependence of $\Sigma(\mathbf{k}, \omega)$ to be quite small prompting the locality feature of the self-energy. Very similar behavior is seen for other \mathbf{k} -points of the BZ and also for the matrix elements corresponding to Ni $d_{3z^2-r^2}$ orbitals. The local self-energy $\Sigma_{loc}(\omega)$ can be evaluated as an integral over all \mathbf{k} -points, and its frequency dependence is shown in Fig. 2 by small circles. We conclude that there is a close agreement between $\Sigma_{loc}(\omega)$ and $\Sigma(\mathbf{k}, \omega)$.

A pole-like behavior for the self-energy at frequencies around 2 eV is also seen in our LDA+FLEX calculation. Those poles are led to additional resonances in the single-particle Green functions that cannot be obtained using static mean DFT based approaches. The imaginary part of the self-energy nearly diverges indicating strongly damped excitations. Those resonances are usually hard to associate with actual energy bands.

We further utilize our LDA+FLEX(RPA) method to evaluate the spin fluctuation mediated pairing interaction. The Fermi surface is triangularized onto small areas described by about 6,000 Fermi surface momenta for which the matrix elements of scattering between the Cooper pairs are calculated using the approach of Ref. [39]. The linearized BCS gap equation is then exactly diagonalized and the set of eigenstates is obtained for both singlet ($S = 0$) and triplet ($S = 1$) Cooper pairs. The highest eigenvalue λ represents the physical solution and the eigenvector corresponds to superconducting energy gap $\Delta_S(\mathbf{k}j)$ where \mathbf{k} is the Fermi surface momentum and j numerates the Fermi surface sheets.

We now analyze the behavior of $\Delta_S(\mathbf{k}j)$ corresponding to two highest eigenvalues λ as a function of the Fermi momentum using the values of $U = 3eV$ and $J = 0.5eV$. They are related to the spin singlet states and Fig.3 a)

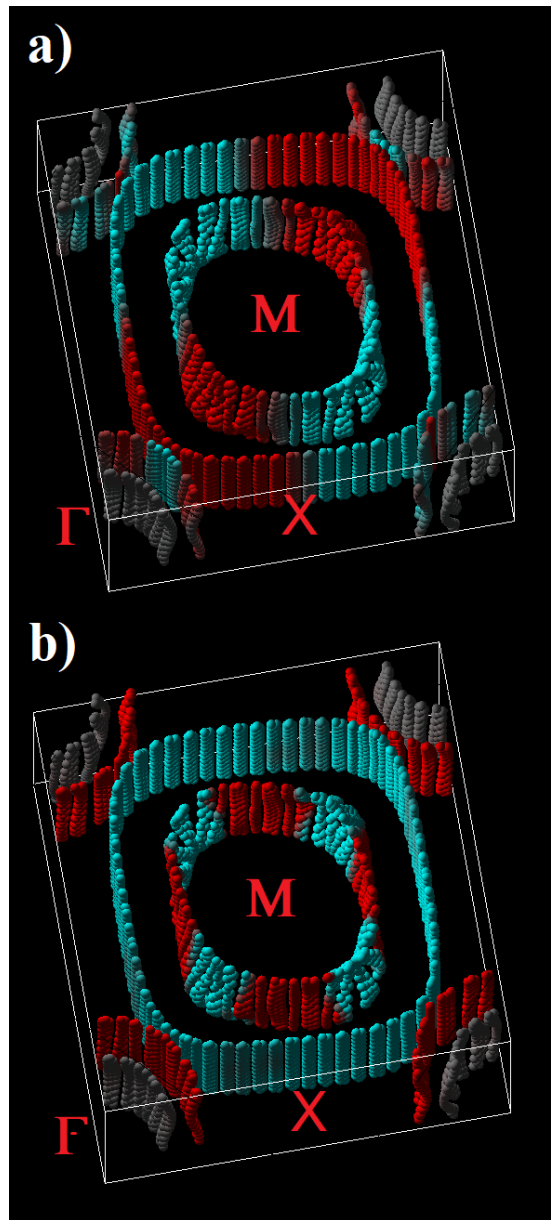


FIG. 3: Calculated superconducting energy gap $\Delta(\mathbf{k})$ for singlet pairing in $\text{La}_3\text{Ni}_2\text{O}_7$ using numerical solution of the linearized BCS gap equation with the pairing interaction evaluated using LDA+FLEX(RPA) approach. Blue/red color corresponds to the negative/positive values of $\Delta(\mathbf{k})$, while the values around zero are colored in gray. Case a) corresponds to the highest eigenstate with d_{xy} symmetry and b) is the next highest with the s_{\pm} symmetry.

and b) show the highest and the next highest eigenstates, respectively. One can see that the most favorable eigenstate $\Delta_{S=0}(\mathbf{k}j)$ shows the behavior of a d-wave with xy symmetry (zeroes pointing along k_x and k_y directions). The plot distinguishes negative/positive values of Δ by blue/red colors while zeroes of the gap function are colored in grey as, for example, the case of the La pocket seen around Γ point. This result is interesting because it

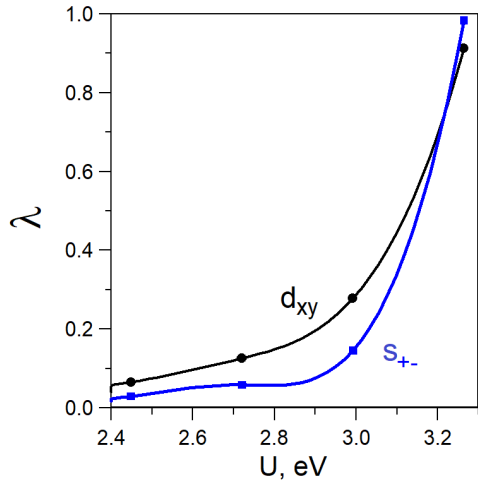


FIG. 4: Calculated dependence of two highest eigenvalues λ corresponding to d_{xy} and s_{\pm} symmetries of the linearized BCS equation as a function of the on-site Hubbard interaction U for d-electrons of Ni in $\text{La}_3\text{Ni}_2\text{O}_7$. Large values of λ are seen for the values of U close to the magnetic instability.

differs from the predicted behavior in cuprates with their $d_{x^2-y^2}$ symmetry and also from iron pnictides with their s_{\pm} behavior. The Fermi surface nesting however is quite strong for both BZ edges at $(1/2,0,0)$ and $(1/2,1/2,0)$ points which results in a delicate competition between the two spin density wave instabilities.

Fig.3 (b) shows the behavior of the second highest eigenstate. Here we clearly resolve sign changing energy gap values for different sheets of the Fermi surface corresponding to the s_{\pm} symmetry. This behavior was recently discussed in several model calculations[19, 20, 22, 26, 29–31], and found explicitly using the RPA calculations with the two-orbital bilayer model [27, 28]. We can reproduce the result of such favored s_{\pm} pairing state when performing our own tight-binding calculations using parameters given in Ref. [22, 23] instead of full density functional calculation of energy bands and wave functions for $\text{La}_3\text{Ni}_2\text{O}_7$.

To gain further insight we vary the parameter U slightly between the values 2.5 and 3.5 eV and extract from the BCS gap equation the highest eigenstates and their symmetries as a function of U . This plot is shown in Fig.4 where one can see that the $\lambda_{d_{xy}}$ corresponding to the d_{xy} symmetry dominates slightly in this range of U 's except for its small region where $\lambda_{s_{\pm}}$ grows rapidly once we approach the spin density wave instability.

Finally, we analyze the behavior of the spin susceptibility that is responsible for the spin fluctuational pairing. Since the BCS approximation assumes that the superconducting pairing K operates for the electrons residing at the Fermi surface only, it can be considered as the static ($\omega = 0$) value for the dynamically resolved interaction: $K(\mathbf{q}, \omega) = I + I\chi(\mathbf{q}, \omega)I$. Here I is the static on-site

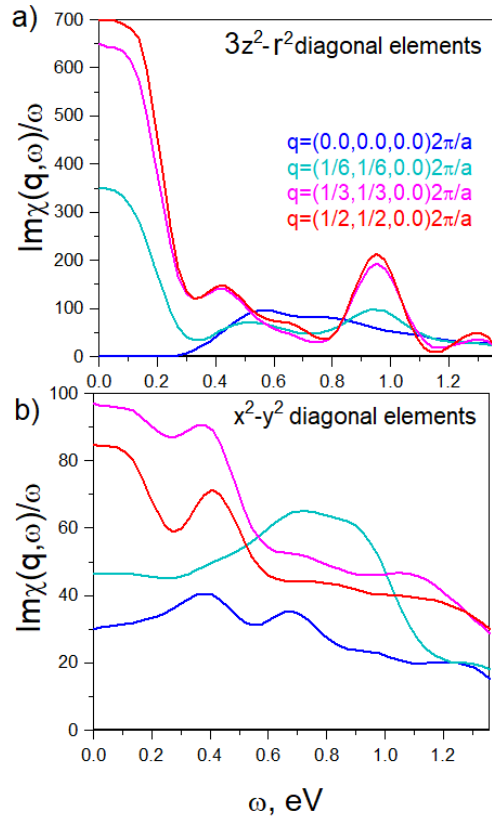


FIG. 5: Calculated imaginary part of spin susceptibility weighted by ω^{-1} in $\text{La}_3\text{Ni}_2\text{O}_7$ plotted as a function of frequency for several wave vectors q transverse from the Γ to M point of the BZ and for the largest diagonal elements of the spin susceptibility that we find for Ni $d_{x^2-y^2}$ (plot a) and Ni $d_{3z^2-r^2}$ (plot b) orbitals.

bare interaction matrix that incorporates U and J while $\chi(\mathbf{q}, \omega)$ is the interacting susceptibility matrix. As a result of the Kramers–Kronig transformation, $\text{Re}K(\mathbf{q}, 0)$ can be expressed via the inverse frequency moment of its imaginary part, $\text{Im}K(\mathbf{q}, \omega)/\omega$, that is further proportional to the imaginary part of the spin susceptibility weighted by ω^{-1} . Thus, the frequency resolution of the spin fluctuational spectrum can be easily analyzed by plotting the function $\text{Im}\chi(\mathbf{q}, \omega)/\omega$. We present this data in Fig.5. The spin susceptibility is the matrix which has four orbitals corresponding to various d-electron states and also two sites corresponding to two NiO_2 planes within the unit cell. We plot the data as a function of frequency for several wave vectors \mathbf{q} traversing along Γ – M line of the BZ and for the largest diagonal elements of the spin susceptibility that we find for Ni $d_{x^2-y^2}$ and Ni $d_{3z^2-r^2}$ orbitals. The spin fluctuational spectrum is primarily located at small frequencies and spans the region until $\approx 0.5\text{eV}$ or so. It exhibits significant momentum dependence which grows toward the edge of the BZ which indicates that the spin fluctuations are primarily

of antiferromagnetic character. Despite the long range antiferromagnetic order is absent in $\text{La}_3\text{Ni}_2\text{O}_7$, this result is quite similar to cuprates and iron based materials where doping is served to suppress the long range magnetic order.

In conclusion, we used recently developed LDA+FLEX method to study spin fluctuational mechanism of superconductivity in recently discovered $\text{La}_3\text{Ni}_2\text{O}_7$ under pressure. Based on this procedure, the superconducting scattering matrix elements between the Cooper pairs have been evaluated numerically, and the linearized BCS gap equation was exactly diagonalized. Our main result is the predicted d_{xy} symmetry for the most favorable eigenstate of the superconducting order parameter although the symmetry s_{\pm} proposed in a series of recent works was found to lie in close proximity. Since both symmetries can be distinguished by the presence/absence of nodes in the gap function, it should be straightforward to sort this out with currently on-going experiments.

-
- [1] Danfeng Li, Kyuho Lee, Bai Yang Wang, Motoki Osada, Samuel Crossley, Hye Ryoung Lee, Yi Cui, Yasuyuki Hikita & Harold Y. Hwang, Superconductivity in an infinite-layer nickelate, *Nature* **572**, 624 (2019).
- [2] Hualei Sun, Mengwu Huo, Xunwu Hu, Jingyuan Li, Zengjia Liu, Yifeng Han, Lingyun Tang, Zhongquan Mao, Pengtao Yang, Bosen Wang, Jinguang Cheng, Daoxin Yao, Guang-Ming Zhang, Meng Wang, Signatures of superconductivity near 80 K in a nickelate under high pressure, *Nature* **621**,493-498 (2023).
- [3] J. Choisnet, R.A. Evarestov, I.I. Tupitsyn and V.A. Veryazov, Investigation of the chemical bonding in Nickel mixed oxides from electronic structure calculations, *J. Phys. Chem. Solids* **157**, 1839 (1996).
- [4] M.J. Martínez-Lope, M.T. Casais, J.A. Alonso, Stabilization of Ni^{1+} in defect perovskites $\text{La}(\text{Ni}_{1-x}\text{Al}_x)\text{O}_{2+x}$ with 'infinite-layer' structure, *J. Alloys and Compounds* **275**, 109 (1998)
- [5] M. A. Hayward, M. A. Green, M. J. Rosseinsky, and J. Sloan, Sodium Hydride as a Powerful Reducing Agent for Topotactic Oxide Deintercalation: Synthesis and Characterization of the Nickel(I) Oxide LaNiO_2 , *J. Am. Chem. Soc.* **121**, 8843 (1999).
- [6] A. Ikeda, T. Manabe, M. Naito, Improved conductivity of infinite-layer LaNiO_2 thin films by metal organic decomposition, *Physica C* **495**, 134 (2013).
- [7] K.-W. Lee and W.E. Pickett, Infinite-layer LaNiO_2 : Ni^{1+} is not Cu^{2+} , *Phys. Rev. B* **70**, 165109 (2004).
- [8] V. I. Anisimov, D. Bukhvalov, and T. M. Rice, Electronic structure of possible nickelate analogs to the cuprates, *Phys. Rev. B* **59**, 7901 (1999).
- [9] D. Li, B. Y. Wang, K. Lee, S. P. Harvey, M. Osada, B. H. Goodge, L. F. Kourkoutis, H. Y. Hwang, Superconducting Dome in $\text{Nd}_{1-x}\text{Sr}_x\text{NiO}_2$ Infinite Layer Films, *Phys. Rev. Lett.* **125**, 027001 (2020).
- [10] Shengwei Zeng, Chi Sin Tang, Xinmao Yin, Changjian Li, Mengsha Li, Zhen Huang, Junxiong Hu, Wei Liu, Ganesh Ji Omar, Hariom Jani, Zhi Shiuh Lim, Kun Han, Dongyang Wan, Ping Yang, Stephen John Pennycook, Andrew T.S. Wee, and Ariando Ariando, Phase diagram and superconducting dome of infinite-layer $\text{Nd}_{1-x}\text{Sr}_x\text{NiO}_2$ thin films, *Phys. Rev. Lett.* **125**, 147003 (2020).
- [11] M. Osada, B Y. Wang, B. H. Goodge, K. Lee, H. Yoon, K. Sakuma, D. Li, M. Miura, L. F. Kourkoutis, H. Y. Hwang, A superconducting praseodymium nickelate with infinite layer structure, *Nano Lett.* **20**, 5735 (2020).
- [12] C. C. Tsuei and J. R. Kirtley, Pairing symmetry in cuprate superconductors, *Rev. Mod. Phys.* **72**, 969 (2000).
- [13] D. J. Scalapino, A common thread: The pairing interaction for unconventional superconductors, *Rev. Mod. Phys.* **84**, 1383 (2012).
- [14] P. A. Lee, N. Nagaosa, and X.-G. Wen, Doping a Mott insulator: Physics of high-temperature superconductivity, *Rev. Mod. Phys.* **78**, 17 (2006).
- [15] For a review, see, e.g, G. Kotliar, S. Y. Savrasov, K. Haule, V. S. Oudovenko, O. Parcollet, C.A. Marianetti, *Rev. Mod. Phys.* **78**, 865, (2006).
- [16] V. Pardo and W. E. Pickett, Metal-insulator transition, in layered nickelates $\text{La}_3\text{Ni}_2\text{O}_{7-\delta}$ ($\delta = 0.0, 0.5, 1$), *Phys. Rev. B* **83**, 245128 (2011).
- [17] X. Chen, P. Jiang, J. Li, Z. Zhong, and Y. Lu, Critical charge and spin instabilities in superconducting $\text{La}_3\text{Ni}_2\text{O}_7$, arXiv:2307.07154.
- [18] For a review, see, e.g., Theory of the Inhomogeneous Electron Gas, edited by S. Lundqvist and S. H. March (Plenum, New York, 1983).
- [19] V. Christiansson, F. Petocchi, and P. Werner, Correlated electronic structure of $\text{La}_3\text{Ni}_2\text{O}_7$ under pressure, *Phys. Rev. Lett.* **131**, 206501 (2023).
- [20] D. A. Shilenko and I. V. Leonov, Correlated electronic structure, orbital-selective behavior, and magnetic correlations in double-layer $\text{La}_3\text{Ni}_2\text{O}_7$ under pressure, *Phys Rev B.* **108**, 125105 (2023).
- [21] F. Lechermann, J. Gondolf, S. Boetzel, and I. M. Eremin, Electronic correlations and superconducting instability in $\text{La}_3\text{Ni}_2\text{O}_7$ under high pressure, *Phys. Rev. B* **108**, L201121 (2023).
- [22] Z. Luo, X. Hu, M. Wang, W. Wu, and D.-X. Yao, Bilayer two-orbital model of $\text{La}_3\text{Ni}_2\text{O}_7$ under pressure, *Phys. Rev. Lett.* **131**, 126001 (2023).
- [23] Y. Zhang, L.-F. Lin, A. Moreo, and E. Dagotto, Electronic structure, orbital-selective behavior, and magnetic tendencies in the bilayer nickelate superconductor $\text{La}_3\text{Ni}_2\text{O}_7$ under pressure, *Phys. Rev. B* **108**, L180510 (2023)
- [24] W. Wu, Z. Luo, D.-X. Yao, and M. Wang, Charge Transfer and Zhang-Rice Singlet Bands in the Nickelate Superconductor $\text{La}_3\text{Ni}_2\text{O}_7$ under Pressure, arXiv:2307.05662.
- [25] Y. Shen, M. Qin, and G.-M. Zhang, Effective bilayer model Hamiltonian and density-matrix renormalization group study for the high-Tc superconductivity in $\text{La}_3\text{Ni}_2\text{O}_7$ under high pressure, *Chinese Physical Letters* **40**, 127401 (2023).
- [26] Y. Gu, C. Le, Z. Yang, X. Wu, and J. Hu, Effective model and pairing tendency in bilayer Ni-based superconductor $\text{La}_3\text{Ni}_2\text{O}_7$, arXiv:2306.0727
- [27] Y. Zhang, L.-F. Lin, A. Moreo, T. A. Maier, and E. Dagotto, Structural phase transition, s_{\pm} -wave pairing and magnetic stripe order in the bilayered nickelate superconductor $\text{La}_3\text{Ni}_2\text{O}_7$ under pressure,

- arXiv:2307.15276.
- [28] Y.-B. Liu, J.-W. Mei, F. Ye, W.-Q. Chen, and F. Yang, The $s\pm$ -Wave Pairing and the Destructive Role of Apical-Oxygen Deficiencies in $\text{La}_3\text{Ni}_2\text{O}_7$ Under Pressure, arXiv:2307.10144.
- [29] Q. Qin and Y.-f. Yang, High-Tc superconductivity by mobilizing local spin singlets and possible route to higher T_c in pressurized $\text{La}_3\text{Ni}_2\text{O}_7$, Phys. Rev. B **108**, L140504 (2023).
- [30] Q.-G. Yang, D. Wang, and Q.-H. Wang, Possible $s\pm$ -wave superconductivity in $\text{La}_3\text{Ni}_2\text{O}_7$, Phys. Rev. B **108**, L140505 (2023).
- [31] Y.-H. Tian, Y. Chen, J.-M. Wang, R.-Q. He, and Z.-Y. Lu, Correlation Effects and Concomitant Two-Orbital $s\pm$ -Wave Superconductivity in $\text{La}_3\text{Ni}_2\text{O}_7$ under High Pressure, arXiv:2308.09698.
- [32] D. J. Scalapino, E. Loh, Jr., and J. E. Hirsch, d-wave pairing near a spin-density-wave instability, Phys. Rev. B **34**, 8190 (1986).
- [33] K. Miyake, S. Schmitt-Rink, and C. M. Varma, Spin-fluctuation-mediated even-parity pairing in heavy-fermion superconductors, Phys. Rev. B **34**, 6554 (1986).
- [34] S. Doniach and S. Engelsberg, Low-Temperature Properties of Nearly Ferromagnetic Fermi Liquids Phys. Rev. Lett. **17**, 750 (1966).
- [35] N. F. Berk and J. R. Schrieffer, Effect of Ferromagnetic Spin Correlations on Superconductivity, Phys. Rev. Lett. **17**, 433 (1966).
- [36] N. E. Bickers, D. J. Scalapino and S. R. White, Con-
serving Approximations for Strongly Correlated Electron Systems: Bethe-Salpeter Equation and Dynamics for the Two-Dimensional Hubbard Model, Phys. Rev. Lett. **62**, 961 (1966).
- [37] B. Menge and E. Müller-Hartmann, The Hubbard model at high dimensions: self-consistent weak coupling theory, Z. Phys. B: Cond. Mat. **82**, 237 (1991).
- [38] S. Y. Savrasov, G. Resta, X. Wan, Local self-energies for V and Pd emergent from a nonlocal LDA+FLEX implementation, Phys. Rev. B **97**, 155128 (2018).
- [39] Griffin Heier, Calculated Spin Fluctuational Pairing Interaction in $\text{HgBa}_2\text{CuO}_4$ using LDA+FLEX Method, Sergey Y. Savrasov, arXiv:2311.10030.
- [40] V. I. Anisimov, F. Aryasetiawan and A. I. Lichtenstein, First-principles calculations of the electronic structure and spectra of strongly correlated systems: the LDA+U method, J. Phys. Condens. Mat. **9**, 767 (1997).
- [41] D. J. Van Harlingen, Phase-sensitive tests of the symmetry of the pairing state in the high-temperature superconductors—Evidence for $d_{x^2-y^2}$ symmetry, Rev. Mod. Phys. **67**, 515 (1995).]
- [42] Z. Zhang, M. Greenblatt, and J.B. Goodenough, Synthesis, Structure, and Properties of the Layered Perovskite $\text{La}_3\text{Ni}_2\text{O}_{7-\delta}$, Journal of Solid State Chemistry, **108**, 402-409 (1994).
- [43] S. Y. Savrasov, Linear-response theory and lattice dynamics: A muffin-tin-orbital approach, Phys. Rev. B **54**, 16470 (1996).